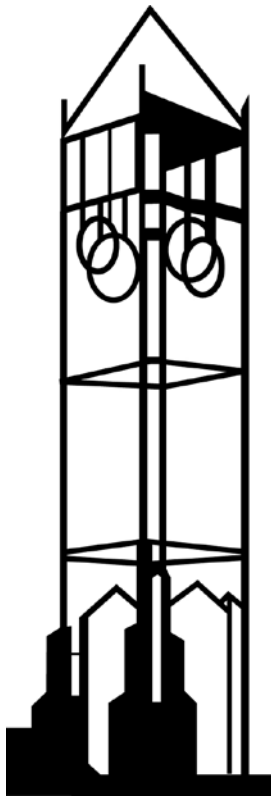


Testing Institutional Arrangements Via Agent-Based Modeling: A U.S. Electricity Market Example

Hongyan Li, Junjie Sun, Leigh Tesfatsion



Working Paper No. 10001
January 2010
Revised on February 2010

IOWA STATE UNIVERSITY
Department of Economics
Ames, Iowa, 50011-1070

Iowa State University does not discriminate on the basis of race, color, age, religion, national origin, sexual orientation, gender identity, sex, marital status, disability, or status as a U.S. veteran. Inquiries can be directed to the Director of Equal Opportunity and Diversity, 3680 Beardshear Hall, (515) 294-7612.

Testing Institutional Arrangements via Agent-Based Modeling: A U.S. Electricity Market Application

Hongyan Li, Junjie Sun, and Leigh Tesfatsion

Abstract Many critical goods and services in modern-day economies are produced and distributed through complex institutional arrangements. Agent-based computational economics (ACE) modeling tools are capable of handling this degree of complexity. In concrete support of this claim, this study presents an ACE test bed designed to permit the exploratory study of restructured U.S. wholesale power markets with transmission grid congestion managed by locational marginal prices (LMPs). Illustrative findings are presented showing how spatial LMP cross-correlation patterns vary systematically in response to changes in the price responsiveness of wholesale power demand when wholesale power sellers have learning capabilities. These findings highlight several distinctive features of ACE modeling: namely, an emphasis on process rather than on equilibrium; an ability to capture complicated structural, institutional, and behavioral real-world aspects (micro-validation); and an ability to study the effects of changes in these aspects on spatial and temporal outcome distributions.

1 Introduction

Modern economies depend strongly on large-scale institutions for the production and distribution of critical goods and services, such as electric power, health care, credit, and education. The performance of these institutions in turn depends in complicated ways on the structural constraints restricting feasible activities, on the rules governing participation, operation, and oversight, and on the behavioral disposi-

Hongyan Li, ABB Inc., Raleigh, NC, USA, e-mail: hongyan.li@us.abb.com · Junjie Sun, Office of the Comptroller of the Currency, U.S. Treasury, Washington D.C. 20219 USA, e-mail: junjie.sun@occ.treas.gov · Leigh Tesfatsion (Corresponding Author), Economics Department, Iowa State University, Ames, IA 50011-1070 USA, e-mail: tesfatsi@iastate.edu · To appear in H. Dawid and W. Semmler (Eds.), *Computational Methods in Economic Dynamics*, Springer, 2011.

tions of human participants. To be useful and informative, institutional studies need to take proper account of all three elements.

Agent-based computational economics (ACE) modeling is well suited for undertaking institutional studies. ACE modeling begins with assumptions about “agents” and their interactions and then uses computer simulation to generate histories that reveal the dynamic consequences of these assumptions. The agents in ACE models can range from passive structural features with no cognitive function to individual and group decision makers with sophisticated learning and communication capabilities. ACE researchers use controlled experimentation to investigate how large-scale effects arise from the micro-level interactions of dispersed agents, starting from variously specified initial conditions.

In particular, ACE researchers take a culture-dish approach to the study of institutional designs. The first step is to develop a computational world that incorporates the salient aspects of the institutional design, along with relevant structural constraints, and that is populated with cognitive agents endowed with realistic behavioral dispositions and learning capabilities. The second step is to specify initial conditions for the computational world. The final step is to permit the computational world to evolve over time driven solely by agent interactions, with no further intervention from the modeler. Two basic questions are typically addressed. First, does the institutional design promote efficient, fair, and orderly social outcomes over time, despite possible attempts by cognitive agents to game the design for their own advantage? Second, under what conditions might the design give rise to adverse unintended consequences?

Introductory discussions focusing on the applicability of ACE modeling for economic research in general can be found in Refs. [1, 2]. Annotated pointers to extensive ACE institutional research can be found at the ACE homepage [3]. The focus of this latter research runs the gamut from macroeconomic policy rules to the microeconomic procurement processes of individual firms.

In this study we apply the ACE approach to a meso-level institutional design problem: namely, exploration of the performance characteristics of wholesale power markets with transmission grid congestion managed by locational marginal prices (LMPs). Under this pricing system, electric power is priced at wholesale in accordance with the location and timing of its injection into, or withdrawal from, the transmission grid.

Our basic framework of analysis is an ACE wholesale power market test bed (“AMES”) developed by a group of researchers at Iowa State University [4]. Illustrative findings are presented from AMES experiments showing how spatial LMP cross-correlation patterns vary systematically in response to changes in the price responsiveness of wholesale power demand when wholesale power sellers have learning capabilities. For example, it is shown how the strategic supply offers of the pivotal sellers whose supply is needed to meet total fixed (price-insensitive) demand strongly influence the LMPs at neighboring locations as well as the LMPs at their own locations. An important policy implication of this finding is that the exercise of market power at any one location can have substantial adverse spill-over effects on prices at other locations, particularly when total demand is largely fixed.

Section 2 provides a brief overview of restructuring efforts for the U.S. electric power industry that have led to the widespread adoption of LMP pricing. Section 3 describes the key features of AMES. An experimental design is outlined in Section 4 for testing the spatial cross-correlation patterns arising among LMPs under systematically varied demand conditions when wholesale power sellers have learning capabilities. Section 5 presents AMES-generated findings for this experimental design. These findings are compared with empirical LMP data for the U.S. Midwest wholesale power market in Section 6. Concluding remarks are provided in Section 7.

2 Study Context: U.S. Restructured Wholesale Power Markets

The U.S. electric power industry is currently undergoing substantial changes in both its *structure* (ownership and technology aspects) and its *architecture* (operational and oversight aspects). These changes involve attempts to move the industry away from highly regulated markets with administered cost-based pricing and towards competitive markets in which prices more fully reflect supply and demand forces.

The goal of these changes is to provide industry participants with better incentives to control costs and introduce innovations. The process of enacting and implementing policies and laws to bring about these changes has come to be known as *restructuring*.

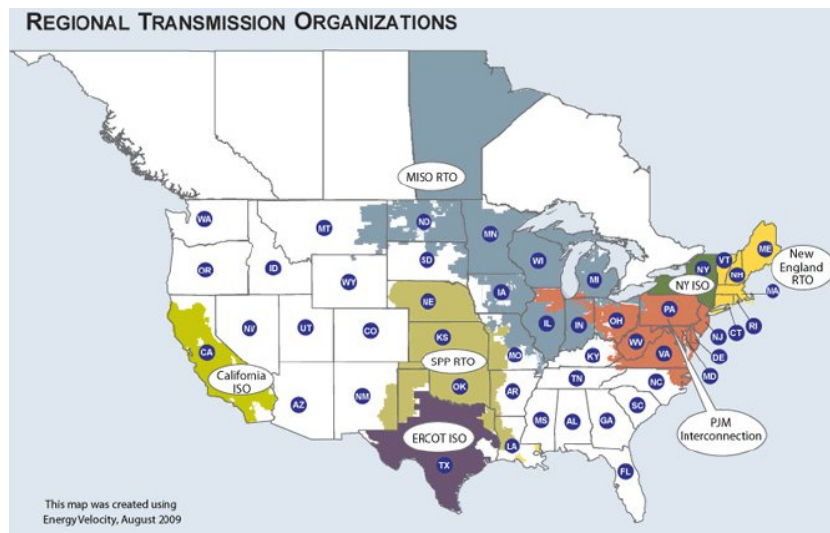


Fig. 1 U.S. energy regions that have adopted FERC's wholesale power market design. Source: www.ferc.gov/market-oversight/mkt-electric/overview.asp

In 2003 the U.S. Federal Energy Regulatory Commission (FERC) recommended the adoption of a common market design for U.S. wholesale power markets [5]. As indicated in Figure 1, and elaborated in [6], versions of this design have now been implemented in U.S. energy regions in the Midwest (MISO), New England (ISO-NE), New York (NYISO), the Mid-Atlantic states (PJM), California (CAISO), the Southwest (SPP), and Texas (ERCOT).

A core feature of FERC’s design is a reliance on *locational marginal prices (LMPs)* to manage transmission grid congestion. Under this pricing system, the price (LMP) charged to wholesale buyers and received by wholesale sellers at a particular grid bus at a particular point in time is the least cost to the system of providing an additional increment of power at that bus at that time.

A key fact about LMPs is that congestion arising on any transmission grid branch necessarily results in separation between the LMPs at two or more grid buses. Previous studies have derived analytical expressions for LMPs at a point in time, conditional on given grid, demand, and supply conditions; see, for example, [7] and [8]. These studies highlight the critical roles played by transmission grid branch constraints and generator production capacity limits in the determination of LMPs. In addition, numerous researchers have empirically investigated the autocorrelation patterns in LMPs as part of price forecasting studies; see, for example, [9]. To our knowledge, however, no previous research has focused on the spatial cross-correlation patterns deliberately or inadvertently induced in LMPs by strategically learning power traders.

This study uses controlled experiments for a 5-bus test case to explore spatial cross-correlation patterns induced in LMPs under systematically varied conditions for the price-sensitivity of wholesale power demand when generation companies have learning capabilities. All experiments were conducted using Version 2.05 of the AMES Wholesale Power Market Test Bed [4], a Java software package developed by H. Li, J. Sun, and L. Tesfatsion. The key features of AMES used in this study are explained in the following section.

3 AMES Wholesale Power Market Test Bed

AMES(V2.05) captures key features of wholesale power market operations in U.S. energy regions operating under FERC’s wholesale power market design [5]. These key features are listed in Figure 2 and briefly described below.¹

The AMES(V2.05) wholesale power market operates over an AC transmission grid starting with hour H00 of day 1 and continuing through hour H23 of a user-specified maximum day. AMES includes an *Independent System Operator (ISO)* and a collection of energy traders consisting of *Load-Serving Entities (LSEs)* $j = 1, \dots, J$

¹ For a more detailed description of AMES, including pointers to tutorials, manuals, and downloadable code, see [4, 10]. AMES is an acronym for *Agent-based Modeling of Electricity Systems*. Annotated pointers to other agent-based electricity research can be accessed at [11].

- **Traders**
 - ▣ LSEs (bulk-power buyers)
 - ▣ GenCos (bulk-power sellers with *learning capabilities*)
- **Independent System Operator (ISO)**
 - ▣ Day-ahead hourly scheduling via *bid/offer-based DC OPF*
 - ▣ System reliability assessments
- **Two-settlement process**
 - ▣ *Day-ahead market* (double auction, financial contracts)
 - ▣ *Real-time market* (settlement of differences)
- **AC transmission grid**
 - ▣ LSEs & GenCos located at user-specified buses across the transmission grid
 - ▣ Congestion managed via *Locational Marginal Pricing (LMP)*.

Fig. 2 Architecture of the AMES Wholesale Power Market Test Bed.

and *Generation Companies (GenCos)* $i = 1, \dots, I$ distributed across the buses of the transmission grid.

The objective of the not-for-profit ISO is the maximization of *Total Net Surplus (TNS)* subject to transmission constraints and GenCo operating capacity limits. In an attempt to attain this objective, the ISO operates a day-ahead energy market settled by means of *locational marginal prices (LMPs)*.

Hourly demand bid for each LSE j = **Fixed demand bid + Price-sensitive demand bid**

- Fixed demand bid = p_{Lj}^F (MWs)
- Price-sensitive demand bid = Linear demand function for real power p_{Lj}^S (MWs) over a purchase capacity interval:

$$D_j(p_{Lj}^S) = c_j - 2d_j p_{Lj}^S$$

$$0 \leq p_{Lj}^S \leq \text{SLMax}_j$$

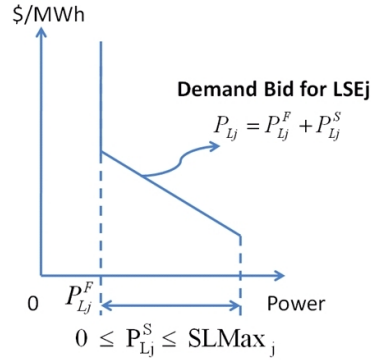


Fig. 3 AMES LSE demand bids consist of fixed and price-sensitive parts.

The objective of each LSE j is to secure for itself the highest possible daily net earnings through purchases of power in the day-ahead market and resale of this power to retail customers. During the morning of each day D , each LSE j reports a *demand bid* to the ISO for the day-ahead market for day $D+1$. Each demand bid consists of two parts: fixed demand (i.e., a 24-hour load profile) that can be sold

downstream at a regulated rate to retail customers with flat-rate pricing contracts; and 24 price-sensitive inverse demand functions, one for each hour, reflecting price-sensitive demand (willingness to pay) by retail customers with real-time pricing contracts. Figure 3 illustrates the form of a demand bid for a particular hour H . LSEs have no learning capabilities; demand bids for LSEs are user-specified at the beginning of each simulation run.

The objective of each GenCo i is to secure for itself the highest possible daily net earnings through the sale of power in the day-ahead market. GenCos have learning capabilities.² During the morning of each day D , each GenCo i uses its current “action choice probabilities” to choose a supply offer from its action domain AD_i to report to the ISO for use in all 24 hours of the day-ahead market for day $D+1$. As depicted in Figure 4, this *supply offer* consists of a reported marginal cost function $MC_i^R(p_{Gi}) = a_i^R + 2b_i^R p_{Gi}$ defined over a reported operating capacity interval $[Cap_i^L, Cap_i^{RU}]$. GenCo i ’s ability to vary its choice of a supply offer from AD_i permits it to adjust the ordinate a_i^R , slope $2b_i^R$, and upper operating capacity limit Cap_i^{RU} for its reported marginal cost function in an attempt to increase its daily net earnings.

Hourly supply offer for each GenCo i = **Reported** linear marginal cost function over a **reported** operating capacity interval for real power p_{Gi} (in MWs):

$$MC_i^R(p_{Gi}) = a_i^R + 2b_i^R p_{Gi}$$

$$Cap_i^L \leq p_{Gi} \leq Cap_i^{RU}$$

GenCos can learn to report **higher-than-true** marginal costs and/or to report **lower-than-true** maximum capacity.

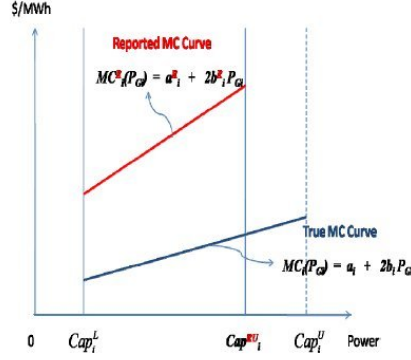


Fig. 4 AMES GenCos with learning capabilities report strategic supply offers to the ISO.

After receiving demand bids from LSEs and supply offers from GenCos during the morning of day D , the ISO determines and publicly posts hourly LMP and dispatch levels for the day-ahead market for day $D+1$. These hourly outcomes are determined via *Security-Constrained Economic Dispatch (SCED)* formulated as bid/offer-based DC optimal power flow (OPF) problems with approximated TNS objective functions based on reported rather than true GenCo costs. Grid congestion is managed by the inclusion of congestion cost components in LMPs. At the end

² A detailed presentation of GenCo learning is given below in Section 4.2.1.

of each day D the ISO settles the day-ahead market for day $D+1$ by receiving all purchase payments from LSEs and making all sale payments to GenCos based on the LMPs for the day-ahead market for day $D+1$, collecting the difference as *ISO net surplus*. The activities of the ISO on a typical day D are depicted in Figure 5.

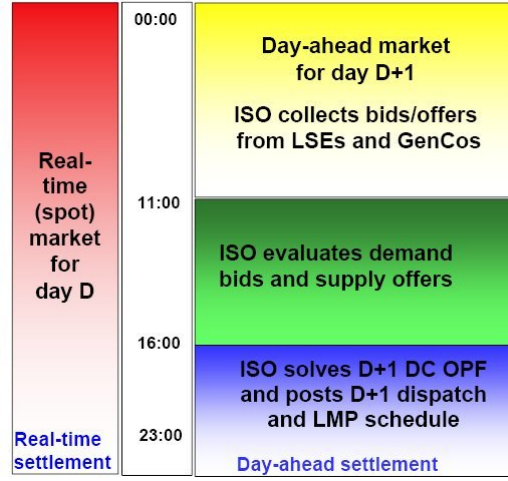


Fig. 5 AMES ISO activities during a typical day D .

Each GenCo i at the end of each day D uses stochastic reinforcement learning to update the action choice probabilities currently assigned to the supply offers in its action domain AD_i , taking into account its day- D settlement payment (“reward”). In particular, if GenCo i ’s supply offer on day D results in a relatively good reward, GenCo i increases the probability it will choose to report this same supply offer on day $D+1$, and conversely.

There are no system disturbances (e.g., weather changes) or shocks (e.g., line outages). Consequently, the dispatch levels determined on each day D for the day-ahead market for day $D+1$ are carried out as planned without need for settlement of differences in the real-time market.

4 Experimental Design

As detailed below, our experimental design is based on a multi-period version of a static 5-bus test case commonly used in ISO business practices manuals and training programs to illustrate market operations. Two treatment factors are selected for the experimental design. The first treatment factor is the degree to which GenCos can learn to exercise *economic capacity withholding*, i.e., the reporting of higher-than-true marginal costs. The second treatment factor is the degree to which LSEs

report fixed versus price-sensitive demand bids, an increasingly important issue as pressures increase for more demand response in wholesale power markets [12, 13].

Three key issues are highlighted in this experimental design. First, given fixed demands, how are bus LMPs affected by the introduction of learning capabilities for the GenCos that permit them to strategically adjust their supply offers over time? Second, given fixed demands, how do network effects and the strategically reported supply offers of the learning GenCos affect the spatial cross-correlations exhibited by bus LMPs? Third, how do the spatial cross-correlations for bus LMPs change in response to systematic increases in demand-bid price sensitivity?

4.1 Benchmark Dynamic 5-Bus Test Case

Our experimental design is anchored by a *benchmark dynamic 5-bus test case* described in full detail in Li et al. [14]. This benchmark case is characterized by the following structural, institutional, and behavioral conditions:

- The wholesale power market operates over a 5-bus transmission grid as depicted in Figure 6, with branch reactances, locations of LSEs and GenCos, and initial hour-0 LSE fixed demand levels adopted from a static 5-bus test case [15] developed for ISO training purposes.

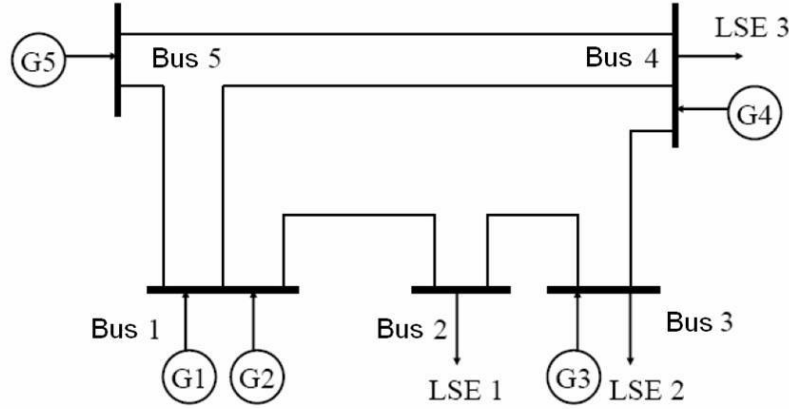


Fig. 6 Transmission grid for the benchmark dynamic 5-bus test case.

- True GenCo cost and capacity attributes are as depicted in Figure 7. GenCos range from GenCo 5, a relatively large coal-fired baseload unit with low marginal operating costs, to GenCo 4, a relatively small gas-fired peaking unit with relatively high marginal operating costs.

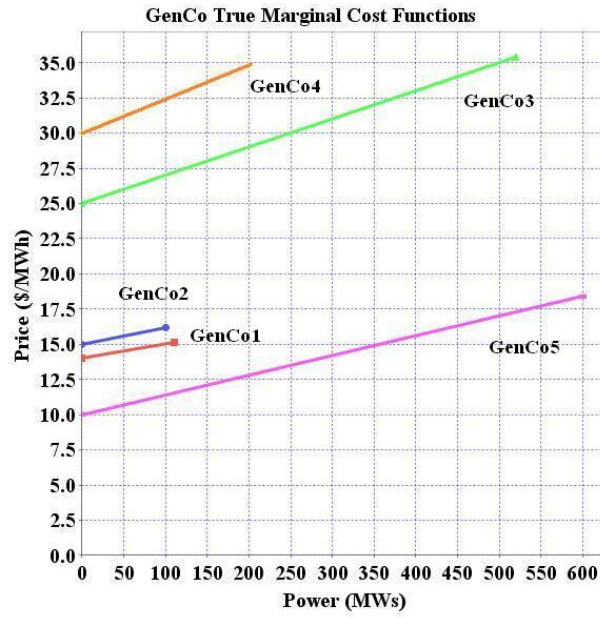


Fig. 7 GenCo true marginal cost functions and true capacity attributes for the benchmark dynamic 5-bus test case.

- Demand is 100% fixed (no price sensitivity) with LSE daily fixed-demand profiles adopted from a case study presented in Shahidehpour et al. [16, p. 296-297]. As depicted in Figure 8, hourly load varies from light (hour H04) to peak (hour H17).

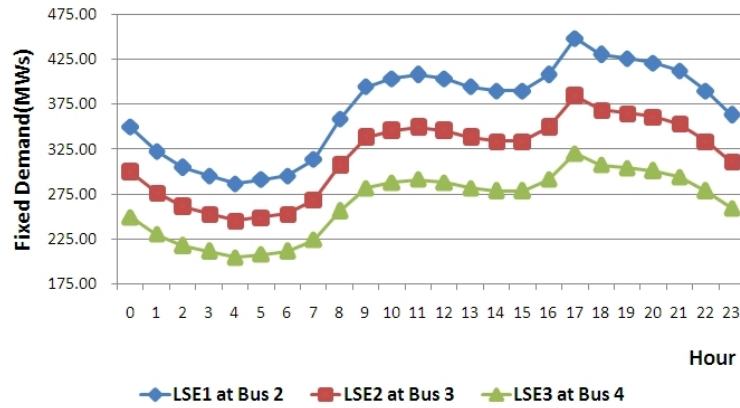


Fig. 8 Fixed demand (load profiles) for the benchmark dynamic 5-bus test case.

- GenCos are non-learners, meaning they report supply offers to the ISO that convey their true marginal cost functions and true operating capacity limits.

4.2 Learning Treatments

Each GenCo i has available an *action domain* AD_i consisting of a finite number of possible supply offers. For the study at hand, a *supply offer* for any GenCo i takes the form of a reported marginal cost function $MC_i^R(p_{Gi}) = a_i^R + 2b_i^R p_{Gi}$ that can be summarized by a vector $s_i^R = (a_i^R, b_i^R)$ determining its ordinate a_i^R and slope $2b_i^R$; see Figure 4.³

The action domain AD_i is tailored to GenCo i 's own particular true cost and capacity attributes. In particular, AD_i only contains reportable marginal cost functions $MC_i^R(p_{Gi})$ lying on or above GenCo i 's true marginal cost function $MC_i(p_{Gi}) = a_i + 2b_i p_{Gi}$, and AD_i always contains this true marginal cost function. However, the action domains are constructed so as to ensure equal cardinalities and similar densities across all GenCos to avoid favoring some GenCos over others purely through action domain construction.⁴

In learning treatments, each GenCo makes daily use of stochastic reinforcement learning to adjust its supply offers in pursuit of increased daily net earnings. As detailed below in Section 4.2.1, GenCo learning is implemented by means of a variant of a stochastic reinforcement learning algorithm developed by Roth and Erev [17, 18] based on human-subject experiments, hereafter referred to as the *VRE learning algorithm*.

For experimental treatments with GenCo VRE learning, we use 30 pseudo-random number seed values to initialize 30 distinct runs, each 1000 simulated days in length.⁵ To control for random effects, outcomes are then reported as mean values across all 30 runs.

4.2.1 VRE Learning Algorithm

This section describes how an arbitrary GenCo i goes about using the VRE learning algorithm to select supply offers s_i^R from its action domain AD_i to report to the ISO for the day-ahead market on successive days D , starting from an initial day $D=1$. As will be seen below, the only relevant attribute of AD_i for implementation of VRE learning is that it has finite cardinality. Consequently, letting $M_i \geq 1$ denote the

³ In the present study it is assumed for simplicity that GenCos only strategically report the ordinate and slope values for their marginal cost functions. They always truthfully report their upper operating capacity limits Cap^U .

⁴ A detailed explanation of this action domain construction can be found in [14, Appendix B].

⁵ These 30 seed values, together with all parameter value settings used for action domain construction and implementation of the VRE learning algorithm, are provided in the input data file for the 5-bus test case included with the AMES(V2.05) download [4].

cardinality of AD_i , it suffices to index the supply offers (“actions”) in AD_i by $m = 1, \dots, M_i$.

The *initial propensity* of GenCo i to choose action $m \in AD_i$ is given by $q_{im}(1)$ for $m = 1, \dots, M_i$. AMES(V2.05) permits the user to set these initial propensity levels to any real numbers. However, the assumption used in this study is that GenCo i ’s initial propensity levels are all set equal to some common value $q_i(1)$, as follows:

$$q_{im}(1) = q_i(1) \text{ for all actions } m \in AD_i \quad (1)$$

Now consider the beginning of any day $D \geq 1$, and suppose the current propensity of GenCo i to choose action m in AD_i is given by $q_{im}(D)$. The *choice probabilities* that GenCo i uses to select an action for day D are then constructed from these propensities using the following commonly used Gibbs-Boltzmann transformation:

$$p_{im}(D) = \frac{\exp(q_{im}(D)/T_i)}{\sum_{j=1}^{M_i} \exp(q_{ij}(D)/T_i)}, \quad m \in AD_i \quad (2)$$

In (2), T_i is a *temperature parameter* that affects the degree to which GenCo i makes use of propensity values in determining its choice probabilities. As $T_i \rightarrow \infty$, then $p_{im}(D) \rightarrow 1/M_i$, so that in the limit GenCo i pays no attention to propensity values in forming its choice probabilities. On the other hand, as $T_i \rightarrow 0$, the choice probabilities (2) become increasingly peaked over the particular actions m having the highest propensity values $q_{im}(D)$, thereby increasing the probability that these actions will be chosen.

At the end of day D , the current propensity $q_{im}(D)$ that GenCo i associates with each action m in AD_i is updated in accordance with the following rule. Let m' denote the action *actually* selected and reported into the day-ahead market by GenCo i in day D . Also, let $NE_{im'}(D)$ denote the *actual* daily net earnings (revenues minus avoidable costs) attained by GenCo i at the end of day D as its settlement payment for all 24 hours of the day-ahead market for day $D+1$.⁶

Then, for each action m in AD_i ,

$$q_{im}(D+1) = [1 - r_i]q_{im}(D) + \text{Response}_{im}(D), \quad (3)$$

where

$$\text{Response}_{im}(D) = \begin{cases} [1 - e_i] \cdot NE_{im'}(D) & \text{if } m = m' \\ e_i \cdot q_{im}(D) / [M_i - 1] & \text{if } m \neq m', \end{cases} \quad (4)$$

⁶ At the beginning of any planning period, a GenCo’s *avoidable costs* refer to the costs it can avoid during the period by shutting down production and possibly taking other actions (e.g., asset re-use or re-sale). In order for production to proceed, revenues from production should at least cover avoidable costs. In the present study the GenCos do not incur start-up/shut-down or no-load costs, and all of their asset expenditures are assumed to be *sunk costs* (not recoverable by re-use or re-sale). Consequently, the *avoidable costs* $VC_i(p_{Gi}^*)$ for each GenCo i associated with a real power production level p_{Gi}^* in any given hour H is the integral of its true marginal cost function $MC_i(p_{Gi}) = a_i + 2b_i p_{Gi}$ over the interval from 0 to p_{Gi}^* .

and $m \neq m'$ implies $M_i \geq 2$. The introduction of the *recency parameter* r_i in (3) acts as a damper on the growth of the propensities over time. The *experimentation parameter* e_i in (4) permits reinforcement to spill over to some extent from a chosen action to other actions to encourage continued experimentation with various actions in the early stages of the learning process.

4.2.2 Calibration of VRE Learning Parameters

As a prelude to conducting experiments with GenCo VRE learning for the dynamic 5-bus test case, we calibrated each GenCo's VRE learning parameter settings to its particular choice environment. We first set common "sweet spot" values $(r, e) = (0.04, 0.96)$ across the GenCos for the recency and experimentation parameters r_i and e_i in (3) and (4) based on the dynamic 5-bus test case analysis conducted by Pentapalli [19]. Given this (r, e) setting, we then conducted intensive parameter sweeps to determine individual "sweet spot" settings for each GenCo i 's initial propensity $q_i(1)$ in (1) and temperature parameter T_i in (2).

More precisely, regarding the latter step, we defined two derived VRE learning parameters (α_i, β_i) for each GenCo i as follows. We proxied GenCo i 's daily net earnings aspirations in normalized form at the beginning of the initial day 1 by constructing the ratio

$$\alpha_i = \frac{q_i(1)}{\text{MaxDNE}_i} \quad (5)$$

of GenCo i 's initial propensity $q_i(1)$ in (1) to an approximate valuation $\text{MaxDNE}_i = [24 \cdot \text{MC}_i(\text{Cap}_i^U) \cdot \text{Cap}_i^U]$ for GenCo i 's maximum possible daily net earnings. We also defined the ratio

$$\beta_i = \frac{q_i(1)}{T_i} \quad (6)$$

of $q_i(1)$ in (1) to GenCo i 's temperature parameter T_i in (2). We then conducted an intensive set of experiments for the dynamic 5-bus test case under alternative specifications for (α, β) , set commonly across the GenCos, with LSE demand maintained at 100% fixed ($R=0.0$)

Figure 9 displays a 3D visualization for the mean total GenCo daily net earnings on day 1000 resulting under the variously tested specifications for (α, β) . Two interesting findings are immediately evident. First, the specification for (α, β) substantially affects GenCo net earnings outcomes. Second, the highest net earnings are associated with "sweet spot" (α, β) combinations that lie along a nonlinear ridge line ranging from $(\alpha, \beta)=(1, 100)$ in the northwest corner to $(\alpha, \beta)=(1/24, 2)$ in the south-central region.

The particular sweet-spot specification $(\alpha, \beta) = (1, 100)$ is used in all of the learning experiments reported below in Section 5.

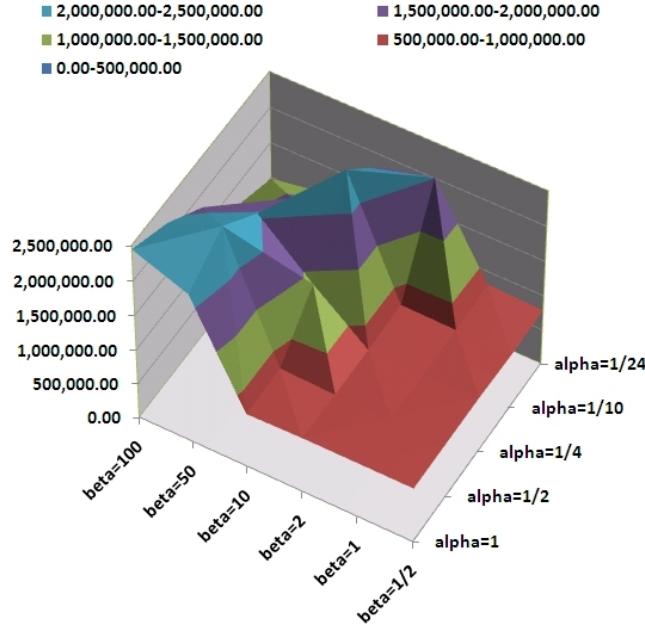


Fig. 9 A 3D depiction of mean outcomes for total GenCo daily net earnings on day 1000 for the dynamic 5-bus test case with GenCo VRE learning and 100% fixed LSE demand ($R=0.0$) under alternative settings for the derived VRE learning parameters (α, β).

4.3 Demand Treatments

The linearity of the LSEs' price-sensitive demand bids implies that price-elasticity of demand varies all along the plots of these functions. Hence, elasticity cannot easily be used to parameterize their sensitivity to price.

To investigate the effects of changes in LSE demand-bid price sensitivity both with and without GenCo VRE learning, we first defined the R-ratio

$$R_j(H, D) = \frac{SLMax_j(H, D)}{[p_{Lj}^F(H, D) + SLMax_j(H, D)]} \quad (7)$$

The numerator of (7) denotes LSE j 's maximum potential price-sensitive demand $SLMax_j(H, D)$ for hour H of the day-ahead market in day $D+1$; see Figure 3. The denominator of (7) denotes LSE j 's maximum potential total demand for hour H of the day-ahead market in day $D+1$, i.e., the sum of its fixed demand and maximum potential price-sensitive demand. Figure 10 illustrates the construction of the R-ratio (7) for the special cases $R=0.0$, $R=0.5$, and $R=1.0$.

We next set all of the LSE fixed demands $p_{Lj}^F(H, D)$ to their positive benchmark-case values $BP_{Lj}^F(H)$ (differing by hour but not by day) and all of the maximum

For LSE j in Hour H :

p_{Lj}^F = Fixed demand for real power (MWs)

$SLMax_j$ = Maximum potential price-sensitive demand (MWs)

$$R = SLMax_j / [p_{Lj}^F + SLMax_j]$$

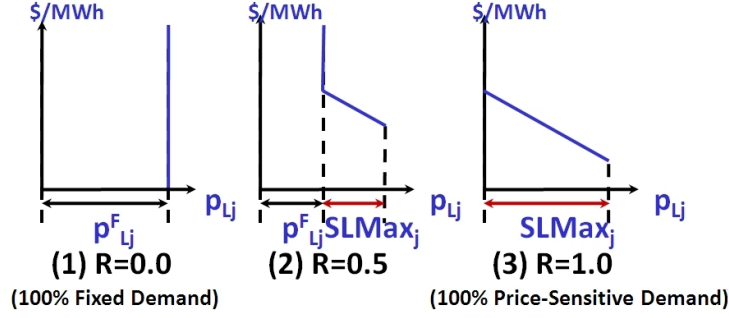


Fig. 10 Illustration of the R-ratio construction for the experimental control of relative demand-bid price sensitivity in each hour H .

potential price-sensitive demands $SLMax_j(H, D)$ to their benchmark-case value 0, thus obtaining a common R-ratio value of $R=0.0$ across all LSEs j for each H and D . We then systematically varied the settings for $p_{Lj}^F(H, D)$ from their benchmark-case values to 0, and the settings for $SLMax_j(H, D)$ from 0 to the positive benchmark-case values $BP_{Lj}^F(H)$ for fixed demand, which resulted in a sequence of common R-ratio values for the LSEs ranging from $R=0.0$ (100% fixed demand) to $R=1.0$ (100% price-sensitive demand).

To prevent confounding effects arising from changes in the ordinate and slope values of the LSE price-sensitive demand bids, these ordinate and slope values were held fixed across all experiments. The specific settings for these fixed ordinate and slope values (along with all benchmark-case values $BP_{Lj}^F(H)$ for LSE fixed demands) are provided in the input data file for the 5-bus test case included with the AMES(V2.05) download [4].

5 Experimental Findings

As shown in Figure 11, GenCo VRE learning and LSE demand-bid price sensitivity critically affect mean LMP outcomes for the dynamic 5-bus test case. In particular, relative to the benchmark (no learning) case, the mean LMP value on day 1000 increases for each given R-ratio value when GenCos are permitted to have VRE learning capabilities. This increase is particularly dramatic for small R-ratio values corresponding to low price-sensitivity of demand.

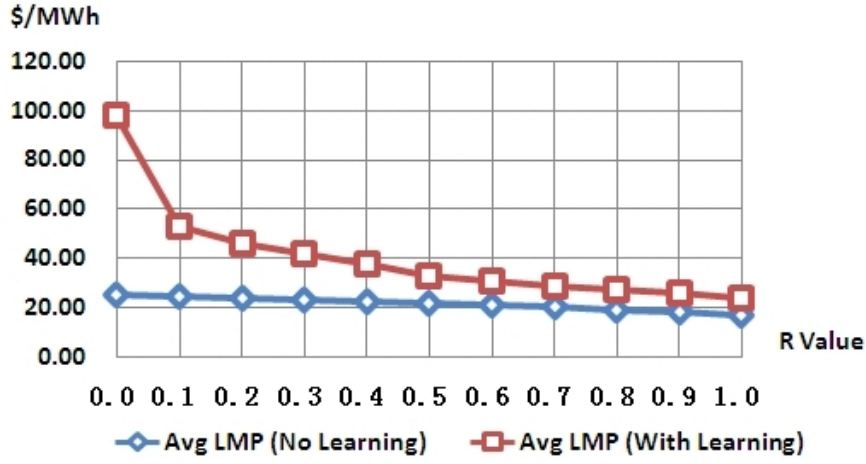


Fig. 11 Mean outcomes for average hourly LMP values on day 1000 for the dynamic 5-bus test case with GenCo VRE learning and LSE demand varying from $R=0.0$ (100% fixed) to $R=1.0$ (100% price sensitive).

However, the mean LMP outcomes reported in Figure 11 do not provide any information regarding the potentially correlated impact of learning and demand-bid price sensitivity on the spatial distribution of LMPs across buses. This section presents experimental findings showing how LMP spatial cross-correlation patterns are systematically affected by changes in GenCo learning capabilities and the price-sensitivity of LSE demand.⁷

5.1 Correlation Experiment Preliminaries

Two types of experimental findings are reported below: (a) pairwise cross-correlations between GenCo reported marginal costs and bus LMPs evaluated at dispatch operating points; and (b) pairwise cross-correlations between bus LMPs evaluated at dispatch operating points.

In each case the cross-correlations are reported at four representative hours from the LSE load profiles depicted in Figure 8: the off-peak hour H04; the shoulder hour H11; the peak-demand hour H17; and the shoulder hour H20. Moreover, for each hour the two types of cross-correlations are reported for three different demand scenarios as characterized by three different settings for the R-ratio. In total, then, 24 distinct cross-correlation treatments ($2 \times 4 \times 3$) are reported below.

⁷ For a fuller presentation of our correlation experiment findings, including detailed comparisons with the no-learning benchmark case, see [14].

Illustrative findings are depicted using correlation diagrams as well as tables. Each correlation diagram uses shape, shape direction, and color to convey information about the sign and strength of the resulting pairwise cross-correlations.

The shapes and shape directions in the correlation diagrams are rough indicators of the patterns observed in the underlying scatter plots for the two random variables whose cross-correlation is under examination. Color is used to reinforce shape and shape direction information.

More precisely, if a scatter plot for two random variables X and Y roughly lies along a straight line, this suggests that X and Y are perfectly correlated. If the line is positively sloped, the indication is perfect positive correlation (1.0); if the line is negatively sloped, the indication is perfect negative correlation (-1.0). The correlation diagrams indicate these possible scatter-plot patterns by means of straight lines that are either forward or backward slanted to indicate positive or negative correlation respectively. Conversely, if the scatter plot for X and Y instead consists of a roughly rectangular cloud of points, this indicates that X and Y are independent of each other, implying zero correlation. The correlation diagrams indicate this scatter-plot pattern by means of full circles. Intermediate to this are scatter plots for X and Y that are roughly elliptical in shape, indicating moderate but not perfect correlation between X and Y . The correlation diagrams indicate this scatter-plot pattern by means of oval shapes that point to the right for positive correlation values and to the left for negative correlation values.

Red-colored shapes indicate positive correlation and blue-colored shapes indicate negative correlation. The intensity of the red (blue) color indicates the degree of the positive (negative) correlation.

5.2 GenCo-LMP Cross-Correlations

Table 1 presents pairwise cross-correlations between GenCo reported marginal costs and bus LMPs for the peak-demand hour H17 of day 1000 for the dynamic 5-bus test case with GenCo VRE learning and 100% fixed LSE demand ($R=0.0$). These cross-correlations indicate positive correlation between GenCo 3 and the LMPs at buses 2-4, negative correlation between GenCo 4 and the LMPs at buses 1 and 5, and strong positive correlation between GenCo 5 and the LMPs at buses 1 and 5. What explains this correlation pattern?

One important explanatory factor is branch congestion and direction of branch power flows during hour H17. As detailed in [14], the branch 1-2 connecting bus 1 and bus 2 is typically congested in every hour under learning. Consequently, buses 2-4 constitute a demand pocket for GenCo 3 located at bus 3. It is therefore not surprising that GenCo 3's reported marginal costs are positively correlated with the LMPs at these demand-pocket buses during the peak-demand hour H17.

In addition, the persistent congestion on branch 1-2 results in a negative correlation between the reported marginal cost for GenCo 4 at bus 4 and the LMPs at buses 1 and 5 during the peak-demand hour H17. This happens because the power injected

Table 1 Pairwise cross-correlations between GenCo reported marginal costs and bus LMPs at the peak-demand hour H17 of day 1000 for the dynamic 5-bus test case with GenCo VRE learning and 100% fixed LSE demand ($R=0.0$).

	LMP 1	LMP 2	LMP 3	LMP 4	LMP 5
G1	0.3136	-0.2244	-0.2143	-0.0718	0.2879
G2	0.4150	0.1344	0.1591	0.4148	0.5042
G3	-0.1164	0.5147	0.5222	0.5363	0.0163
G4	-0.2711	0.4641	0.4625	0.3811	-0.1718
G5	0.9704	-0.3125	-0.2712	0.2293	1.0000

by GenCo 4 during hour H17 substitutes in part for the cheaper power of GenCos 1 and 5 in servicing demand at the demand-pocket buses 2-4. This substitution occurs because GenCos 1 and 5 are located at buses 1 and 5 and hence are semi-islanded behind the congested branch 1-2 during hour H17 as dictated by the directions of branch power flows.

A second important explanatory factor is limits on generation operating capacities during hour H17, which affect the marginal status of the different GenCos.⁸ As is well known (see [8]), the LMP at each bus with a marginal GenCo is given by the reported marginal cost of this GenCo whereas the LMP at each bus without a marginal GenCo is given by a weighted linear combination of the reported marginal costs of the marginal GenCos.

As indicated in Table 2, GenCo 5 located at bus 5 is persistently marginal during the peak-demand hour H17, hence the LMP at bus 5 persistently coincides with GenCo 5's reported marginal cost. This explains the finding in Table 1 of a perfect positive correlation of 1.0 between GenCo 5's reported marginal cost and the LMP at bus 5 during hour H17.

Table 2 Frequency of GenCo marginality across 30 runs measured at four different hours on day 1000 for the dynamic 5-bus test case with GenCo VRE learning and 100% fixed LSE demand ($R=0.0$).

	G1	G2	G3	G4	G5
H04	13%	37%	100%	37%	100%
H11	10%	30%	100%	20%	100%
H17	10%	23%	87%	20%	100%
H20	10%	30%	100%	13%	100%

Table 2 also indicates that no other GenCo is persistently marginal during hour H17. For example, GenCo 3 is dispatched at maximum operating capacity in 13% of the runs due either to a relatively low reported marginal cost by GenCo 3 or a relatively high reported marginal cost by GenCo 4. This non-marginality of GenCo 3 restrains the positive correlation between GenCo 3's reported marginal costs and

⁸ A GenCo is said to be *marginal* if its minimum and maximum operating capacity limits are not binding at its dispatch point.

the LMPs at the demand-pocket buses 2-4 as well as the extent to which power supplied by GenCo 3 can substitute for the power of GenCos 1 and 5 during H17.

The correlation diagram in Figure 12 for the peak-demand hour H17 provides a visualization of the GenCo-LMP cross-correlation findings in Table 1. In particular, it helps to highlight the importance of GenCos 3 and 4 for the determination of LMPs at the demand-pocket buses 2-4, and the importance of GenCo 5 for the determination of LMPs at buses 1 and 5.

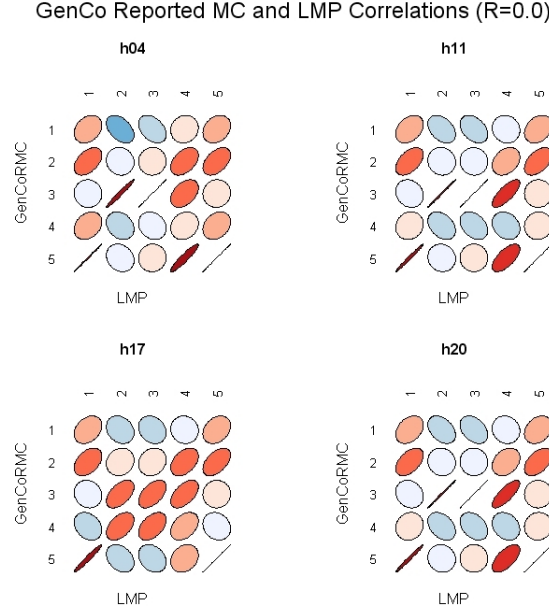


Fig. 12 Pairwise cross-correlations between GenCo reported marginal costs and bus LMPs for hours H04, H11, H17, and H20 on day 1000 for the dynamic 5-bus test case with GenCo VRE learning and 100% fixed LSE demand ($R=0.0$).

The remaining correlation diagrams in Figure 12 depict the GenCo-LMP cross-correlations that arise in the off-peak hour H04, the shoulder hour H11, and the shoulder hour H20. Comparing these results to the results depicted in Figure 12 for the peak-demand hour H17, note that GenCo 3's reported marginal cost is now perfectly positively correlated with the LMP at bus 3 and is strongly positively correlated with the LMPs at its neighboring buses 2 and 4. These changes arise because the substantially lower fixed demand in these three non-peak hours results in the persistent marginality of the relatively large GenCo 3; see Table 2.

Also, in contrast to the peak-demand hour H17, GenCo 4's reported marginal cost is negatively correlated with the LMPs at buses 2 and 3 in the three non-peak hours. This occurs because GenCo 4 is in direct rivalry with the marginal GenCo 3 to supply power to buses 2 and 3 during these non-peak hours. For example, GenCo

4 is dispatched at maximum capacity when its reported marginal cost is relatively low, which then permits GenCo 3 to service residual demand at buses 2 and 3 at a relatively high reported marginal cost.

Figures 13 and 14 report the effects on GenCo-LMP cross-correlations when the R-ratio for measuring relative price-sensitivity of LSE demand is systematically increased first to $R=0.5$ (50% potential price sensitivity) and then to $R=1.0$ (100% price sensitivity). As demand becomes more price sensitive, the LSEs more strongly contract their demand in response to price increases and branch congestion becomes less frequent. This limits the GenCos' ability to profitably exercise economic withholding, i.e., to profitably report higher-than-true marginal costs.

In particular, as R increases, the GenCos with relatively low true marginal costs are advantaged and those with relatively high true marginal costs lose out. This can be seen by comparing the correlation diagrams in Figures 12 through 14. As R increases from $R=0.0$ to $R=1.0$, the relatively cheap GenCo 5 gains increased influence over each bus LMP while the relatively expensive GenCo 3 loses influence over the demand-pocket buses 2 through 4.

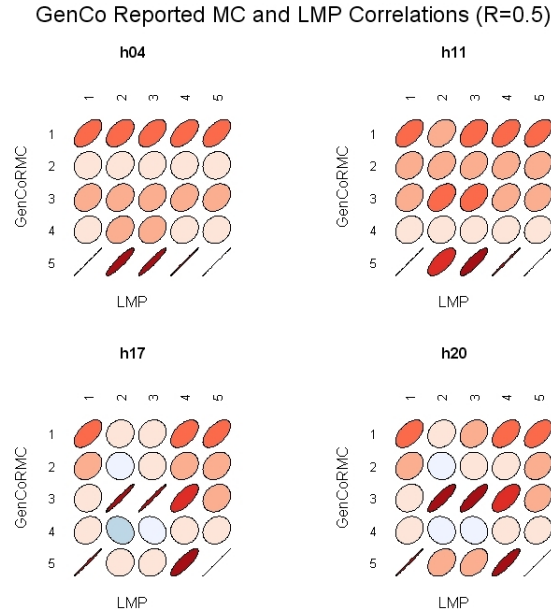


Fig. 13 Pairwise cross-correlations between GenCo reported marginal costs and bus LMPs for hours H04, H11, H17, and H20 on day 1000 for the dynamic 5-bus test case with GenCo VRE learning and 50% fixed LSE potential demand ($R=0.5$).

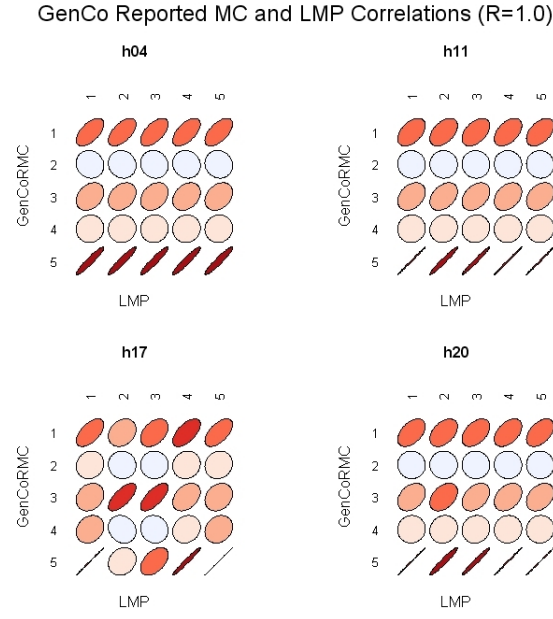


Fig. 14 Pairwise cross-correlations between GenCo reported marginal costs and bus LMPs for hours H04, H11, H17, and H20 on day 1000 for the dynamic 5-bus test case with GenCo VRE learning and 100% price-sensitive LSE demand ($R=1.0$).

5.3 LMP Cross-Correlations

Table 3 reports pairwise cross-correlations for the bus LMPs during the peak-demand hour H17 on day 1000 for the benchmark dynamic 5-bus test case extended to include GenCo VRE learning. Figs. 15 through 17 depict the changes induced in these cross-correlations when the price-sensitivity of demand is systematically increased from $R=0.0$ (100% fixed) to $R=1.0$ (100% price sensitive).

Table 3 Pairwise cross-correlations between bus LMPs at the peak-demand hour H17 of day 1000 for the dynamic 5-bus test case with GenCo VRE learning and 100% fixed LSE demand ($R=0.0$).

	LMP 1	LMP 2	LMP 3	LMP 4	LMP 5
LMP 1	1.0000	-0.5328	-0.4957	-0.0127	0.9704
LMP 2		1.0000	0.9991	0.8530	-0.3125
LMP 3			1.0000	0.8747	-0.2712
LMP 4				1.0000	0.2293
LMP 5					1.0000

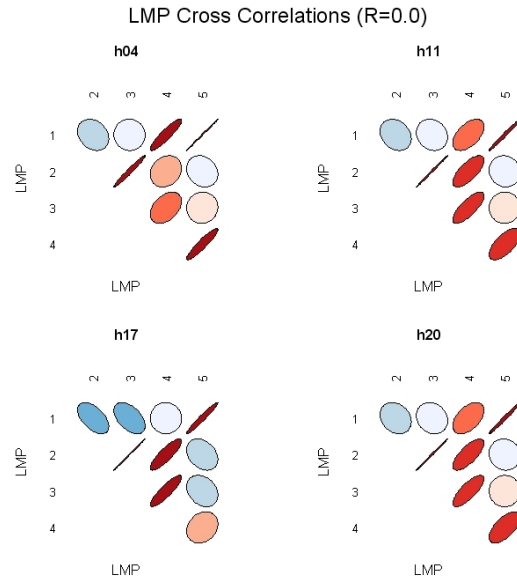


Fig. 15 Pairwise LMP cross-correlations for hours H04, H11, H17, and H20 on day 1000 for the dynamic 5-bus test case with GenCo VRE learning and 100% fixed LSE demand ($R=0.0$).

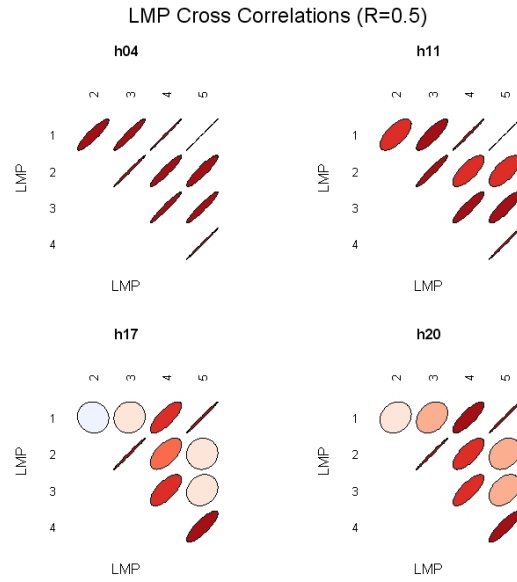


Fig. 16 Pairwise LMP cross-correlations for hours H04, H11, H17, and H20 on day 1000 for the dynamic 5-bus test case with GenCo VRE learning and 50% fixed LSE potential demand ($R=0.5$).

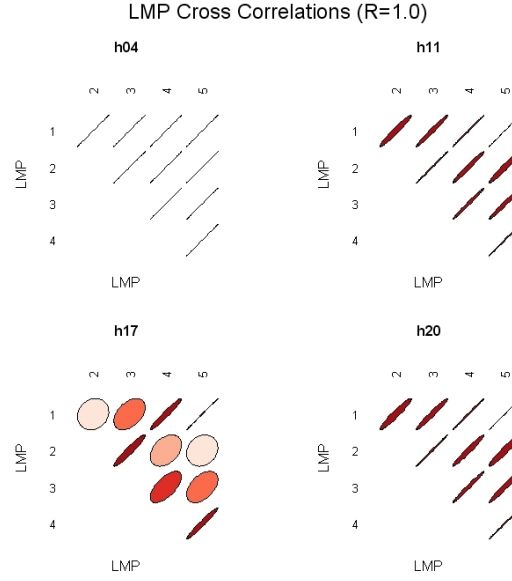


Fig. 17 Pairwise LMP cross-correlations for hours H04, H11, H17, and H20 on day 1000 for the dynamic 5-bus test case with GenCo VRE learning and 100% price-sensitive LSE demand ($R=1.0$).

The main regularity seen in the Table 3 results is that all of the LMP cross-correlations become increasingly positive as R increases. This is particularly true for the non-peak hours H04, H11, and H20 with relatively lower LSE fixed demands.

As R increases, a larger portion of LSE total demand is price sensitive. Consequently, the LSEs are able to exercise more resistance to higher prices through demand contraction, which in turn reduces branch congestion. In the current context, bus LMPs are derived from bid/offer-based DC OPF solutions with zero losses assumed.⁹ Consequently, as congestion diminishes, the LMPs exhibit less separation. In the limit, if all congestion were to disappear, the LMPs would converge to a single uniform price across the grid, which in turn would imply perfect positive correlation among all bus LMPs.

For the non-peak hours H04, H11, and H20, the typical result for the limiting case $R=1.0$ is no branch congestion. Hence, the bus LMPs during these hours—particularly hour H04—are close to being perfectly positively correlated when $R=1.0$. For the peak-demand hour H17, however, the branch 1-2 is typically congested even for $R=1.0$. Consequently, LMP cross-correlations for hour H17 exhibit a strong but not perfect positive correlation.

Another regularity seen in Table 3, and graphically visualized in Figs. 15 through 17, is that the LMP at bus 2 is always strongly positively correlated with the LMP at bus 3. At high R levels, this reflects a lack of branch congestion and hence a lack

⁹ See [20] for a rigorous presentation of this LMP derivation.

of LMP separation. At low R levels, however, the branch 1-2 tends to be congested at all hours. The congestion on branch 1-2 means that the bulk of the demand at the load-only bus 2 must be supplied along branch 3-2 by the large and frequently marginal GenCo 3. This in turn means that the LMP at bus 2 is most strongly influenced by the LMP at bus 3.

6 Empirical Evidence on LMP Cross-Correlations

This section presents LMP cross-correlations calculated using real-world price data. In particular, we focus on LMP determination in a neighborhood of the *MidAmerican Energy Company (MEC)*, the largest utility in Iowa. Through April 2009, MEC was treated as a *Balancing Authority (BA)* in MISO.¹⁰ A BA is responsible for maintaining load-interchange-generation balance and Interconnection frequency support.

From the geographical map depicted in Figure 18, we picked four neighboring BAs of MEC in order to study MEC's effect on their LMPs. These BAs are *Alliant Energy Corporate Services, Inc. (ALTW)*, *Muscatine Power and Water (MPW)*, *Omaha Public Power District (OPPD)*, and *Nebraska Public Power District (NPPD)*. We obtained 24-hour historical data from MISO for the real-time market and day-ahead market LMPs determined for these BAs on August 1, August 3, and September 1 of 2008; see [21]. In particular, for ALTW we used the LMP for the loadzone ALTW.MECB, and for the remaining four BAs we used interface LMPs. We then used these data to calculate pairwise cross-correlations between the LMP reported for MEC and the LMPs reported for its four neighboring BAs.

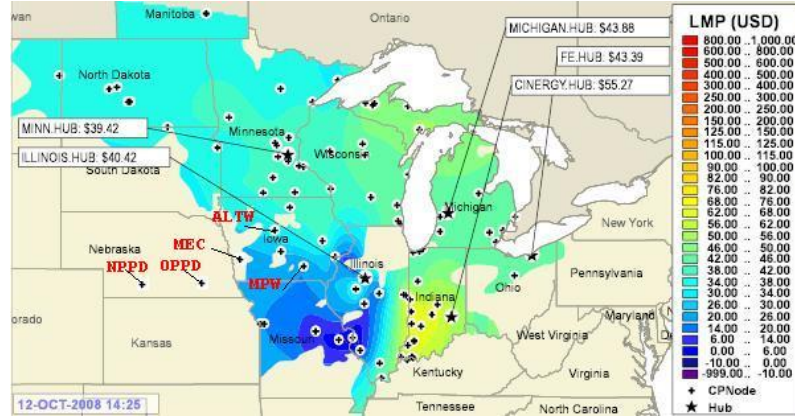


Fig. 18 MidAmerican Energy Company (MEC) Balancing Authority and four neighboring Balancing Authorities in relation to MISO.

¹⁰ On May 1, 2009, MEC filed an application with the Iowa Utilities Board to become a transmission-owning member of MISO.

Table 4 Pairwise cross-correlations between real-time market (RTM) and day-ahead market (DAM) LMPs for the MidAmerican Energy Company (MEC) and four neighboring Balancing Authorities ALTW, MPW, OPPD, and NPPD during three days in 2008.

	DAM 8/1	DAM 8/3	DAM 9/1	RTM 8/1	RTM 8/3	RTM 9/1
MEC-ALTW	0.998	0.999	1.000	0.994	0.974	1.000
MEC-MPW	0.996	0.998	1.000	0.996	0.973	1.000
MEC-OPPD	1.000	0.999	1.000	0.996	0.973	1.000
MEC-NPPD	0.998	0.995	0.998	0.983	0.824	1.000

Table 4 reports our LMP cross-correlation findings. All of the LMP cross-correlations are strongly positive. Since MEC is large, and presumably marginal, this suggests that the supply behavior of the MEC could be spilling over to affect the LMPs at neighboring BAs.

On the other hand, as always, care must be taken to recognize potentially confounding effects in real-world data. As noted above, the LMPs reported by MISO for MEC and its four neighboring BAs are load-weighted prices determined for a loadzone and interfaces and not for a single bus. The strong positive LMP cross-correlations in Table 4 could be a statistical artifact arising from the particular load-weighting method employed. Alternatively, they could indicate a lack of branch congestion during the selected days arising either through happenstance or through deliberate ISO planning.

To differentiate between these various potential explanations for the strong positive correlations in Table 4—GenCo spillover effects, statistical artifact, and lack of congestion—we would need to obtain data on MEC supply offers and branch congestion at an hourly level for the selected test days, as well as data giving individualized bus LMPs. These data are not currently publicly available.

Although agent-based test beds such as AMES can be used to develop interesting hypotheses under simulated scenarios, the real payoff to such development will only come when these hypotheses can be tested more fully against empirical data.

7 Concluding Remarks

In this study we have used an ACE test bed to explore the performance characteristics of wholesale power markets operating under locational marginal pricing in accordance with a market design proposed by the U.S. Federal Energy Regulatory Commission [5]. In particular, we have focused on a novel issue, the extent to which economic capacity withholding by pivotal generation companies with learning capabilities at particular bus locations under variously specified LSE demand conditions has spill-over effects on the prices at neighboring bus locations.

As seen in Section 5, these spill-over effects can be substantial. These spill-over effects thus have practical policy consequences. For example, they greatly complicate efforts to develop and implement effective trigger rules and “reference curves”

for the mitigation of market power in wholesale power markets. As surveyed in Isemonger [22], many of these efforts have focused largely on local price effects.

Although our study focuses on a concrete ACE institutional design application, it illustrates more generally some of the more distinctive capabilities of ACE modeling. First, ACE modeling focuses on the playing out of processes over historical time rather than on the existence of equilibria. Second, the flexible nature of ACE modeling permits researchers to incorporate complicated structural, institutional, and behavioral aspects of actual real world situations. Third, ACE modeling permits researchers to study the effects of changes in these aspects on outcome distributions, both spatially and temporally.

Given these distinctive capabilities, ACE modeling would certainly appear to be a welcome addition to the economist's toolkit, complementing standard analytical and statistical modeling approaches.

Acknowledgements This work has been supported in part by the National Science Foundation under Grant NSF-0527460 and by grants from the ISU Electric Power Research Center.

References

1. L. Tesfatsion, "Agent-Based Computational Economics: A Constructive Approach to Economic Theory," pp. 831–880 in L. Tesfatsion and K. L. Judd (eds.), *Handbook of Computational Economics: Volume 2, Agent-Based Computational Economics*, Handbook in Economics Series, North-Holland/Elsevier, Amsterdam, The Netherlands, 2006.
2. L. Tesfatsion, *Introductory Materials: Agent-Based Computational Economics*, website hosted by the ISU Economics Department, <http://www.econ.iastate.edu/tesfatsi/aintro.htm>
3. L. Tesfatsion, *Agent-Based Computational Economics Homepage*, website hosted by the ISU Economics Department, www.econ.iastate.edu/tesfatsi/ace.htm
4. *AMES Wholesale Power Market Test Bed Homepage*, website hosted by the ISU Economics Department, <http://www.econ.iastate.edu/tesfatsi/AMESMarketHome.htm>
5. FERC, *Notice of White Paper*, U.S. Federal Energy Regulatory Commission, April 2003.
6. P. Joskow, "Markets for power in the united states: An interim assessment," *The Energy Journal*, vol. 27, no. 1, pp. 1–36, 2006.
7. A. J. Conejo, E. Castillo, R. Minguez, and F. Milano, "Locational marginal price sensitivities," *IEEE Transactions on Power Systems*, vol. 20, no. 4, pp. 2026–2033, 2005.
8. T. Orfanogianni and G. Gross, "A general formulation for LMP evaluation," *IEEE Transactions on Power Systems*, vol. 22, no. 3, pp. 1163–1173, 2007.
9. Q. Zhou, L. Tesfatsion, and C.C. Liu, "Scenario generation for price forecasting in restructured wholesale power markets," *IEEE Proceedings, Power Systems & Exposition Conference*, Seattle, WA, March 2009.
10. H. Li and L. Tesfatsion, "The AMES wholesale power market test bed: A computational laboratory for research, teaching, and training," *IEEE Proceedings, Power and Energy Society General Meeting*, Calgary, Alberta, CA, July 2009.
11. L. Tesfatsion, *Agent-Based Computational Economics Research Area: Restructured Electricity Markets*, website hosted by the ISU Economics Department, www.econ.iastate.edu/tesfatsi/aelect.htm
12. L. Lynne Kiesling, "The role of retail pricing in electricity restructuring," pp. 39–62 in A. N. Kleit, *Electric choices: Deregulation and the future of electric power*, Rowman & Littlefield, NY, 2007.

13. FERC, "Assessment of demand response and advance metering," Staff Report, Federal Energy Regulatory Commission, December 2008.
14. H. Li, J. Sun, and L. Tesfatsion, "Separation and volatility of locational marginal prices in restructured wholesale power markets," ISU Econ Working Paper No. 09009, June 2009. www.econ.iastate.edu/research/publications/viewabstract.asp?pid=13075
15. J. Lally, "Financial transmission rights: Auction example," section 6 in *Financial Transmission Rights Draft 01-10-02*, m-06 ed., ISO New England, Inc., January 2002.
16. M. Shahidehpour, H. Yamin, and Z. Li, *Market Operations in Electric Power Systems*, New York, NY: IEEE/Wiley-Interscience, John Wiley & Sons, Inc., 2002.
17. A. E. Roth and E. Ido, "Learning in extensive form games: Experimental data and simple dynamic models in the intermediate term," *Games and Econ. Behavior*, vol. 8, pp. 164–212, 1995.
18. I. Erev and A. E. Roth, "Predicting how people play games with unique mixed-strategy equilibria," *American Economic Review*, vol. 88, pp. 848–881, 1998.
19. Mridul Pentapalli, "A Comparative Study of Roth-Erev and Modified Roth-Erev Reinforcement Learning Algorithms for Uniform-Price Double Auctions" (pdf slides, 6M), M.S. Thesis, Computer Science Department, March 2008.
20. H. Liu, L. Tesfatsion, and A.A. Chowdhury, "Derivation of locational marginal prices for restructured wholesale power markets," *Journal of Energy Markets*, Vol. 2, No. 1, pp. 3–27, 2009.
21. H. Li and L. Tesfatsion, *MISO Energy Project Homepage*, Data section <http://www.econ.iastate.edu/tesfatsi/MISOenergygroup.htm#Data>
22. A. Isemonger, "Conduct and Impact Versus Direct Mitigation," *The Electricity Journal*, Vol. 20, Issue 1, Jan./Feb. 2007, 53–62.